Photosynth Res (2015) 126:449–463
DOI 10.1007/s11120-015-0121-1

REGULAR PAPER

Repetitive light pulse-induced photoinhibition of photosystem I severely affects CO_2 assimilation and photoprotection in wheat leaves

Marek Zivcak[1] · Marian Brestic[1] · Kristyna Kunderlikova[1] · Oksana Sytar[1,2] · Suleyman I. Allakhverdiev[3,4,5]

Received: 22 January 2015 / Accepted: 12 March 2015 / Published online: 1 April 2015

Abstract It was previously found that photosystem I (PSI) photoinhibition represents mostly irreversible damage with a slow recovery; however, its physiological significance has not been sufficiently characterized. The aim of the study was to assess the effect of PSI photoinhibition on photosynthesis in vivo. The inactivation of PSI was done by a series of short light saturation pulses applied by fluorimeter in darkness (every 10 s for 15 min), which led to decrease of both PSI (~60 %) and photosystem II (PSII) (~15 %) photochemical activity. No PSI recovery was observed within 2 days, whereas the PSII was fully recovered. Strongly limited PSI electron transport led to an imbalance between PSII and PSI photochemistry, with a high excitation pressure on PSII acceptor side and low oxidation of the PSI donor side. Low and delayed light-induced NPQ and $P700^+$ rise in *inactivated* samples indicated a decrease in formation of transthylakoid proton gradient (ΔpH), which was confirmed also by analysis of electrochromic bandshift (ECS_t) records. In parallel with photochemical parameters, the CO_2 assimilation was also strongly inhibited, more in low light (~70 %) than in high light (~45 %); the decrease was not caused by stomatal closure. PSI electron transport limited the CO_2 assimilation at low to moderate light intensities, but it seems not to be directly responsible for a low CO_2 assimilation at high light. In this regard, the possible effects of PSI photoinhibition on the redox signaling in chloroplast and its role in downregulation of Calvin cycle activity are discussed.

Keywords PSI photoinactivation · Transthylakoid proton gradient · Non-photochemical quenching · Electrochromic bandshift · P700

Abbreviations

A_{CO_2}	CO_2 assimilation rate
CET	Cyclic electron transport
cyt b_6/f	Cytochrome b_6/f
ECS	Electrochromic shift
ETR	Apparent electron transport rate
F_0	Minimum fluorescence from dark-adapted leaf (PSII centers open)
F'_0	Minimum fluorescence from light-adapted leaf
F_m, F'_m	Maximum fluorescence from dark- or light-adapted leaf respectively (PS II centers closed)
FNR	Ferredoxin $NADP^+$ oxidoreductase
F_v/F_m	Maximum quantum yield of PSII photochemistry
gH^+	Transthylakoid proton conductivity
LED	Light emitting diode
LHC	Light harvesting complex

Electronic supplementary material The online version of this article (doi:10.1007/s11120-015-0121-1) contains supplementary material, which is available to authorized users.

✉ Marian Brestic
marian.brestic@uniag.sk

✉ Suleyman I. Allakhverdiev
suleyman.allakhverdiev@gmail.com

[1] Department of Plant Physiology, Slovak Agricultural University, Tr. A. Hlinku 2, 949 76 Nitra, Slovak Republic

[2] Department of Plant Physiology and Ecology, Taras Shevchenko National University of Kyiv, Volodymyrska St. 64, Kyiv 01601, Ukraine

[3] Institute of Plant Physiology, Russian Academy of Sciences, Botanicheskaya Street 35, Moscow 127276, Russia

[4] Institute of Basic Biological Problems, Russian Academy of Sciences, Pushchino, Moscow Region 142290, Russia

[5] Department of Plant Physiology, Faculty of Biology, M.V. Lomonosov Moscow State University, Leninskie Gory 1-12, Moscow 119991, Russia

NPQ	Non-photochemical quenching
P	P700 absorbance at given light intensity
P700	Primary electron donor of PSI (reduced form)
$P700^+$	Primary electron donor of PSI (oxidized form)
PAM	Pulse-amplitude modulated
PAR	Photosynthetic active radiation
P_m, P'_m	Maximum P700 signal in dark- or light-adapted state
Pmf	Proton motive force
PS I	Photosystem I
PS II	Photosystem II
Q_A	Primary PSII acceptor
Q_A^-/Q_A	Total Redox poise of the primary electron acceptor of PSII ($1 - qP$)
qE	PH dependent energy dissipation
qL	'Lake' model photochemical quenching coefficient
qP	'Puddle' model photochemical quenching coefficient
SP	Saturation light pulse
ΔpH	Transthylakoid pH gradient
ΔpH_{pmf}	Osmotic component of proton motive force
Φ_{NA}	Quantum yield of non-photochemical energy dissipation in PSI due to acceptor side limitation
Φ_{ND}	Quantum yield of non-photochemical energy dissipation in PSI due to donor side limitation
Φ_{NO}	Quantum efficiency of non-regulated energy dissipation in PSII
Φ_{NPQ}	Quantum yield of pH-dependent energy dissipation in PSII
Φ_{PSI}	Effective quantum yield (efficiency) of PSI photochemistry at given actinic light intensity
Φ_{PSII}	Actual quantum yield (efficiency) of PSII photochemistry
$\Delta\psi$	Transmembrane electric potential
$\Delta\psi_{pmf}$	Electric component of proton motive force

Introduction

In oxygenic photosynthesis of plants, photosystem I (PSI) and II (PSII) are the pigment containing reaction centers located in the thylakoid membrane, which are involved in the light reactions of photosynthesis (Barber and Andersson 1994). PSII can split water and use it as a source of electrons, which are transferred along the electron transport chain (including PSI), ultimately reducing $NADP^+$. Proton translocation, which is coupled with electron transport, occurs across the thylakoid membrane from the stroma to the thylakoid lumen. The resulting proton gradient (ΔpH) is utilized in ATP synthesis. In addition to this linear electron transport, cyclic electron transport (CET) around PSI probably also participates in the ΔpH formation (Shikanai 2012, 2014). As CET is not coupled with NADPH accumulation, it may contribute to the photosynthetic flexibility necessary for photoprotection and to ensure the ATP/NADPH output ratio for plant metabolism (Kramer et al. 2003; Kramer and Evans 2011). In addition to ATP synthesis, transthylakoid proton gradient (ΔpH) is needed for activation of non-photochemical quenching by protonating the protein PsbS (Li et al. 2000) and activating the xanthophyll cycle (Demmig-Adams 1990). The proton gradient in thylakoids is also necessary to trigger the ΔpH-dependent regulation of linear electron transport by cytochrome b_6/f, which plays a particularly important role in protecting of PSI against photooxidative damage (Joliot and Johnson 2011). Cyclic electron flow also plays a role in photoprotection of PSI (Bukhov and Carpentier 2004; Miyake 2010). In addition, the changes in activities of both photosystems may contribute to the regulation of linear electron transport, especially in stress conditions (Goltsev et al. 2012; Wang and Chen 2013; Zivcak et al. 2014a, etc.).

PSI is thought to be more resistant to high light than PSII (Powles 1984, Allakhverdiev and Murata 2004, 2008; Murata et al. 2007). It was shown that the PSI reaction center itself is very efficient in dissipating energy as heat (Bukhov and Carpentier 2003). PSI with an intact antenna system is relatively resistant to high light because the antenna proteins are the first target of high light damages. When photoprotection mechanisms become insufficient, the antenna chlorophyll proteins act as fuses: LHCI chlorophylls are degraded while the reaction center photochemical activity is maintained (Alboresi et al. 2009). Anyway, it was shown that isolated PSI could be photoinhibited by high light in the absence of PSII activity (Purcell and Carpentier 1994; Rajagopal et al. 2002, 2003). Examples of PSI photoinhibition in low temperature conditions are well known (Sonoike and Terashima 1994; Sonoike 1996; Scheller and Haldrup 2005). Under physiologically relevant conditions, severe PSI photoinhibition may occur. As an example, Terashima et al. (1994) observed 70–80 % decrease of quantum yield of photosynthetic electron flow through PSI after 5 h chilling of cucumber leaves at 4 °C, at moderate light intensity; the PSII quantum yield decreased only by 20 %. Although the PSI damage in cold-sensitive species use to be more severe (Sonoike 2011), PSI photoinhibition has been shown even in cold-tolerant species such as winter rye (Ivanov et al. 1998) and barley (Tjus and Møller 1998; Tjus et al. 1999), in field conditions, as well (Teicher et al. 2000). However, the recent studies examining the effects of fluctuating light have clearly demonstrated that PSI may be endangered by photoinhibition even at optimum temperature, especially if the linear electron flow is not properly regulated (Suorsa et al. 2012; Grieco et al. 2012; Tikkanen et al. 2012, 2014; Kono et al. 2014).

The mechanism of PSI photoinhibition and recovery has received less attention compared to PSII. Yet, it was shown that the primary reason of PSI photoinactivation is the hydroxyl radicals produced by reaction between hydrogen peroxide and light-reduced iron-sulfur centers of PSI. They trigger the conformational change in the PSI complex, which allows access of a serine-type protease to PsaB (Sonoike et al. 1997). Other studies have indicated that PsaA is also degraded during photoinhibition of PSI (Tjus et al. 1999). It was clearly demonstrated that photoinactivation of PSI runs only in normal (high) oxygen content in the atmosphere, but not in low oxygen (Sonoike and Terashima 1994; Sejima et al. 2014); this supports the mechanism of photoinhibition of PSI by radicals produced on the PSI acceptor side.

PSI recovery was shown to be a very slow process, which may take several days, even under optimal conditions (Sonoike 1996; Teicher et al. 2000; Zhang and Scheller 2004; Zhang et al. 2011), and in some cases, the PSI damage was not completely reversible (Kudoh and Sonoike 2002). Most of the photoinhibited PSI reaction center complexes are not repaired, but degraded after photoinhibition together with its binding chlorophylls (Sonoike 2011). Until stress relief, no or a very slow protein degradation took place. In contrary, when the plants were transferred to non-stressed conditions, damaged PSI cores were completely degraded in a few hours, but the subsequent resynthesis of PSI was still very slow (Kudoh and Sonoike 2002; Zhang and Scheller 2004).

Since PSI damage seems to be irreversible, it may have more severe consequences for plants than PSII photoinhibition. Nevertheless, the physiological significance PSI photoinhibition is still not well known; mainly, because it is usually difficult to distinguish the effects of low PSI activity from other co-occurring effects, caused by cold or other treatments causing PSI damage. Therefore, the method of photo-inactivation developed by C. Miyake's research group from Kobe University, Japan (Sejima et al. 2014) represents a unique way to induce PSI photoinhibition in normal (non-mutant) samples with minimal side effects. The method is based on application of short saturation pulses (SP) (e.g., 300 ms, 10,000 μmol photons m^{-2} s^{-1} or more, every 10 s) in darkness, resulting in gradual PSI inactivation. An advantage of this kind of treatment is that the level of PSI (and PSII) inactivation can be monitored by the device enabling simultaneous measurements of chlorophyll fluorescence and P700 (e.g., DUAL-PAM, Walz, Germany). Up to now, the harmless effect of short saturation light pulses used by PAM devices has been considered to be almost insignificant for photochemical components, although there were some findings on SP-induced PSII photodamage (Shen et al. 1996), but also about photoinactivation of electron transport chain by SP applied in darkness, which was, however, not attributed to PSI photoinhibition (Apostol et al. 2001).

The method of artificial PSI photo-inactivation is based on SP of a very strong light, which far exceeds the naturally occurring light intensities, and thus, it does not attempt to be a direct simulation of what really happens in natural conditions. Anyway, using this method, all changes observed after SP treatment can be attributed solely to the effects of PSI inactivation, almost without undesirable concomitants. Therefore, in our study, we applied a short series of repetitive light pulses (15 min, 90 SP) on wheat leaves in order to investigate the specific effects of PSI-photoinactivation on CO_2 assimilation rate and parameters related to PSI and PSII photochemistry. Our results clearly indicate that PSI photoinhibition may directly affect the photochemical processes, photoprotection and it may cause a significant decrease of CO_2 assimilation. Possible explanations and implications of these findings are discussed.

Material and methods

Plant material and cultivation

The plants of spring wheat (*Triticum aestivum* L.) cv. Corso were used for the experiments. Wheat plants were grown in pots (nine seedlings per pot) with the standard peat substrate, in a growth chamber with artificial light provided by fluorescent tubes (growing conditions: 10/14 h dark/light at 16/20 °C; PAR at leaf level ~300 μmol photons m^{-2} s^{-1}).

Simultaneous measurements of P700 redox state and chlorophyll fluorescence

The PSI and PSII photochemical parameters were measured with a Dual PAM-100 (Walz, Germany) with a ChlF unit and P700 dual wavelength (830/875 nm) unit, as described by Klughammer and Schreiber (1994). SP (15,000 μmol photons m^{-2} s^{-1}), intended primarily for the determination of ChlF parameters were used also for the assessment of the P700 parameters. Prior to the measurements, plants were dark adapted for 15 min in a dark box, and for approximately 2 min in the measuring head. After the determination of F_0, F_m, and P_m, the moderate light intensity (134 μmol photons m^{-2} s^{-1}) was used to start the photosynthetic processes for approximately 10 min (the length and intensity of pre-illumination was tested and shown to be sufficient). After a steady-state was reached, a rapid light curve was triggered (light intensities 14, 21, 30, 45, 61, 78, 103, 134, 174, 224, 281, 347, 438, 539, 668, 833, 1036, 1295, 1602, and 1930 μmol photons m^{-2} s^{-1}; 30 s at each light intensity) with saturation pulse and far-red pulse for F'_0 determination after 30 s at each light intensity. For the calculation of the ChlF parameters, the

following basic values were used: F, F'—fluorescence emission from dark- or light-adapted leaf, respectively; F_0—minimum fluorescence from dark-adapted leaf (PSII centers open); F_m, F'_m—maximum fluorescence from dark- or light-adapted leaf, respectively (PSII centers closed); F'_0—Minimum fluorescence from light-adapted leaf. The ChlF parameters were calculated as follows (Kramer et al. 2004; Baker 2008; Kalaji et al. 2014): the maximum quantum yield of PSII photochemistry, $F_v/F_m = (F_m - F_0)/F_m$; the actual quantum yield (efficiency) of PSII photochemistry, $\Phi_{PSII} = (F_m - F')/F'_m$; non-photochemical quenching, $NPQ = (F_m - F'_m)/F'_m$; 'Puddle' model photochemical quenching coefficient, $qP = (F'_m - F')/(F'_m - F'_0)$. 'Lake' model photochemical quenching coefficient, $qL = qP(F_0/F')$. Quantum efficiency of non-regulated energy dissipation in PSII, $\Phi_{NO} = 1/[NPQ + 1 + qL(F_m/F_0 - 1)]$; quantum yield of pH-dependent energy dissipation in PSII, $\Phi_{NPQ} = 1 - \Phi_{PSII} - \Phi_{NO}$; the redox poise of the primary electron acceptor of PSII, Q_A^-/Q_A total = 1–qP. The fast-relaxing component of NPQ was calculated using measurements after a dark relaxation period (10 min) after high light treatment: $qE = F_m/F'_m - F_m/F''_m$, where F''_m is the maximum fluorescence after dark relaxation following the high light period (Thiele et al. 1997). The apparent electron transport rate of PSII photochemistry was calculated by assuming a leaf absorption of 0.84 and a PSII:PSI ratio of 1:1, $ETR_{PSII} = \Phi_{PSII} \times PAR \times 0.84 \times 0.5$.

For the calculation of the P700 parameters, the following basic values were used: P—P700 absorbance at given light intensity; P_m, P'_m—maximum P700 signal measured using saturation light pulse following short far-red pre-illumination in dark- or light-adapted state. The P700 parameters were calculated as follows (Klughammer and Schreiber 1994): effective quantum yield (efficiency) of PSI photochemistry at given PAR, $\Phi_{PSI} = (P'_m - P)/P_m$; oxidation status of PSI donor side, i.e., the fraction of P700 oxidized at given state, $P700^+/P700$ total $= \Phi_{ND} = P/P_m$; reduction status of PSI acceptor side, i.e., the fraction of overall P700 oxidized in a given state by saturation pulse due to a lack of electron acceptors, $\Phi_{NA} = (P_m - P'_m)/P_m$. In PSI-*inactivated* samples, both measured and original P_m values (measured in the exact same position on leaf prior the PSI inactivation) were used in calculation of P700 parameters. The apparent electron transport rate of PSI photochemistry was calculated by assuming a leaf absorption of 0.84 and a PSII:PSI ratio of 1:1, $ETR_{PSI} = \Phi_{PSI} \times PAR \times 0.84 \times 0.5$.

Measurements of electrochromic bandshift

Non-invasive measurements of absorbance changes denoted as electrochromic bandshift (ECS) were performed with an LED-based spectrophotometer (JTS 10, Biologic, France) following Joliot and Joliot (2002). The difference in exponential decay of the signals measured at 520 nm (ΔA_{520}) and 546 nm ($\Delta A_{520} - \Delta A_{546}$) in first 100 ms was used as a measure of membrane potential (pmf). Measuring flashes were provided by a white LED filtered at 520 (546) nm. The time resolution of the instrument was 10 µs. Prior to taking measurements the sample was pre-illuminated by the artificial white light with intensity ~300 µmol photons m^{-2} s^{-1} for at least 2 h. Then, the leaf was inserted into the leaf holder, and the red light (630 nm, intensity ~200 µmol photons m^{-2} s^{-1}) was applied for 15 min prior to the measurements of ECS decay. After 15 min at given light intensities, the ECS decay was measured at 520 nm by switching off the actinic light. Then, the leaf was pre-illuminated again with the same intensity for 3 min and the same protocol of ECS decay was measured at 546 nm. The signal measured at 546 nm was subtracted from the record measured at 520 nm, which allowed deconvolution of the ECS signal from the absorption changes associated with the redox changes related to the electron flow, e.g., the cytochrome b6f complex (Joliot and Joliot 2002). The parameters derived from ECS decay were calculated according to Sacksteder and Kramer (2000). The amplitude of ECS decay normalized to chlorophyll content will be considered as a measure of proton motive force. The thylakoid H^+ conductivity (gH^+) estimated as the reciprocal value of the halftime of the fast ECS decay in samples adapted to high light. The slow relaxation of ECS signal enabled to recognize the contribution of two components of pmf (ΔpH_{pmf} and $\Delta\Psi_{pmf}$), as described in detail elsewhere (Zivcak et al. 2014b). As the measurement in *control* and *inactivated* samples was done at exactly the same position on the same leaf, no normalization of ECS signal was needed, and hence, the original values of ECS data were used for comparison of treatments.

Measurements of gas exchange

The photosynthetic rate was measured in steady-state conditions and within light response curves using a gasometer (Ciras2, PP-systems, UK). The following conditions were maintained within the measuring head: leaf temperature 20 °C, reference CO_2 content 380 ppm and ambient air humidity. The actinic light was provided by LED light unit (red and blue light LEDs). The measurements consisted from initial induction of photosynthesis at a single light intensity (1000 µmol photons m^{-2} s^{-1}) until stomata were fully open and steady state was reached. Then, the light response curve was applied, starting with record at 1500 µmol photons m^{-2} s^{-1}, continued by stepwise decreasing levels of actinic light (1200, 1000, 800, 600, 500, 400, 300, 200, 142, 122, 100, 79, 56, 45, 25, 0 µmol photons m^{-2} s^{-1}). As the photosynthetic enzyme system was sufficiently activated, time approximately

3 min was sufficient to reach a steady level of measured photosynthetic parameters at each light intensity.

PSI inactivation treatment and design of measurements

Prior the PSI inactivation, all measurements were done, obtaining data presented here as '*control*' (non-inactivated). Then, inactivation was done in the same leaves and at the same position on the leaf (hereinafter '*inactivated*').

PSI inactivation was done using the method developed by C. Miyake's research group (Sejima et al. 2014). SP of red light (300 ms, 15,000 μmol photons m^{-2} s^{-1}) was applied every 10 s in the absence of actinic light (AL) under normal air conditions for 15 min using simultaneous records of chlorophyll fluorescence and P700 parameters, as described above. To ensure a sufficient area of the PSI inactivated leaf sample for gas exchange measurements, two identical PSI inactivation treatments were done, close together, producing 20 mm long inactivated leaf area, which was marked and all subsequent measurements were done exactly in the same position. After PSI inactivation, plants were grown in the same conditions as before treatment.

The complete measurement procedures (chlorophyll fluorescence with P700, ECS records and gas exchange measurements) were done 3 times:

- On the day of the PSI photoinhibition (after min. 2 h in ambient light conditions).
- 1 day after PSI photoinhibition.
- 2 days after PSI photoinhibition.

Moreover, P_m (P700 amplitude) was measured each 2–3 days for next 2 weeks, to monitor recovery of PSI after PSI inactivation.

Data processing and analysis

The measurements of gas exchange, ChlF, and P700 were analyzed from 6 repeated measurements. The mean values ± SEs ($\alpha = 0.05$) are presented here. The statistical significance of differences was assessed using ANOVA followed by the post hoc Tukey HSD test to identify statistically homogenous groups.

Results

PSI inactivation

The inactivation treatment consisted of SP of red light (300 ms, 15,000 μmol photons m^{-2} s^{-1}) applied every 10 s for 15 min, i.e., 90 pulses were applied in each treatment. The repetitive SP led to decrease of both PSII and PSI quantum efficiency (Fig. 1a); however, decrease of Φ_{PSII} (approximately 15–20 %) was much lower than decrease of Φ_{PSI} (approximately 50–60 %). Whereas the Φ_{PSII} was partially recovered a few minutes after frequent SP were stopped, the recovery of Φ_{PSI} was negligible. The decrease of Φ_{PSI} was caused by an increase of acceptor side limitation (Φ_{NA}); the SP did not cause increase of $P700^+$ as the Φ_{ND} was almost nil.

The highest rate of PSI inactivation (rate of decrease of Φ_{PSI}) was approximately 2–3 min after treatment started (Fig. 1b); after 5 min, the PSI inactivation was gradually slowed down. The rate of Φ_{PSII} decrease was the highest at the beginning, then slowly declined.

The maximum photo oxidizable PSI content (P_m), i.e., the maximum amplitude of P700 signal (P_m), is the main criterion for assessment of PSI photoinactivation. The analysis of recovery after PSI photoinhibition (Fig. 1c) shows no PSI recovery in the first 2 days after SP treatment. We can observe a gradual increase of P_m, starting from 4th day, but 12 days after SP treatment, the P_m values were still below the initial level. This confirms that the recovery after PSI photoinhibition used to be a very slow. In contrary, the PSII (indicated by F_0, F_m values) was fully recovered on the second day after SP treatment (Supplementary Fig. 1).

Simultaneous measurements of chlorophyll fluorescence and P700

The effects of PSI inactivation on electron and proton transport-related processes were tested using simultaneous measurements of chlorophyll fluorescence and PSI transmittance in leaf samples exposed to graduated light intensities (Fig. 2).

PSII quantum yield decreased quickly in *inactivated* samples and it was significantly lower compared to values measured before inactivation in all light intensities (Fig. 2a). Light induced increase of quantum yield of ΔpH-dependent non-photochemical quenching (Φ_{NPQ}) was lower in *inactivated* samples compared to *control* (Fig. 2d). As a result of the decrease in Φ_{PSII} and Φ_{NPQ}, we observed very high values of non-regulated (ΔpH-independent) non-photochemical quenching of absorbed light energy (Φ_{NO}), especially in low and moderate light intensities (Fig. 2g). Translating Φ_{PSII} into PSII electron transport rate (Fig. 2j), we can see significantly lower ETR_{PSII} in *inactivated* leaf samples.

The interpretation of P700 records becomes more complicated after PSI inactivation, as the subsequent measurements were not able to detect a fraction of inactivated PSI RCs. To avoid this, we used original values of P_m measured before PSI inactivation in the same place of leaf for calculation of P700 parameters (Fig. 2b, e, h, k).

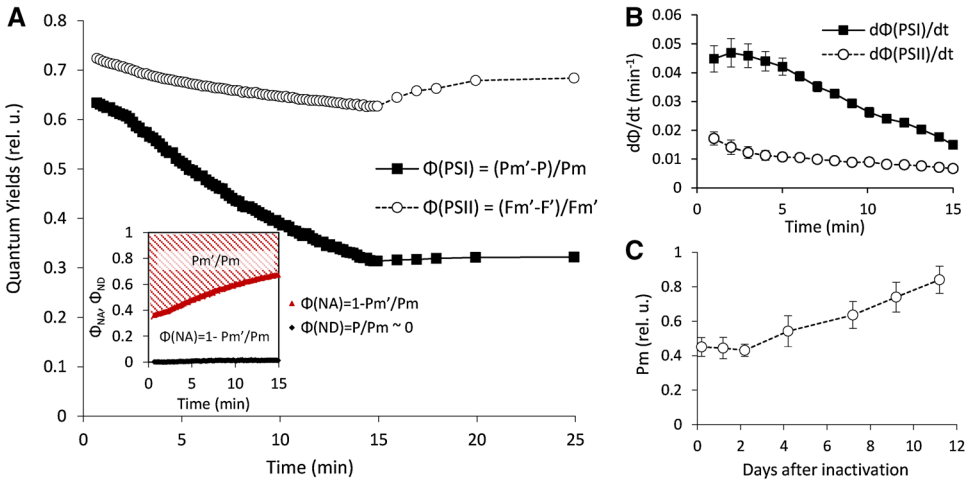

Fig. 1 **a** Example of records of PSI and PSII inactivation within a PSI inactivation procedure: decrease of PSI and PSII quantum yields during exposition of leaf sample to regular SP in the darkness (SP every 10 s for a period of 15 min) followed by 10 min of dark recovery. The small insertion shows the values of Φ_{NA} (increasing) and Φ_{ND} ($\sim$0) during PSI inactivation. The hatched area represents content of photooxidizable PSI, indictated as P'_m/P_m. **b** The rate of PSI and PSII inactivation (dΦ/dt) calculated every minute during the PSI inactivation procedure (average value $\pm$ SE of 6 records). **c** The recovery of PSI (values of P_m related to the values measured before inactivation) after PSI inactivation in 2 weeks following after the PSI inactivation procedure (average value $\pm$ SE of six records)

Thus, we found low values of PSI quantum yield (Φ_{PSI}) even in very low light irradiation, and almost constant Φ_{PSI} with some decrease only at very high light intensities. It indicates that in low light (e.g., 100 µmol photons m^{-2} s^{-1}) only a third of PSI RCs are involved in PSI electron transport in *inactivated* samples compared to *control*. In *control* leaves, there is an initial decrease of Φ_{PSI} followed by subsequent increase, which can be attributed to the startup of cyclic electron flow around PSI. This pattern disappeared from the light response curve of Φ_{PSI} recorded in *inactivated* sample. Values of quantum yield of non-photochemical quenching of PSI caused by the donor side limitation (Φ_{ND}, Fig. 2e) showed much lower accumulation of oxidized P700 related to all PSI RCs ($P700^+/P700_{TOT}$). The values of non-photochemical quenching of PSI caused by acceptor side limitation (Φ_{NA}, Fig. 2h) were very high compared to *control*, but it was caused by the fact, that this parameter involves also the fraction of inactivated PSI. The PSI electron transport rate (Fig. 2k) had a similar trend as ETR_{PSII}. In addition to lower values in *inactivated* samples compared to *control*, there was a high difference also in the level of irradiation which was sufficient to saturate electron transport. The plateau phase after initial steep increase of ETR_{PSI} appeared at $\sim$300 µmol photons m^{-2} s^{-1} in *control* samples, but at $\sim$1.000 µmol photons m^{-2} s^{-1} in *inactivated* samples.

When using the data of complementary PSI quantum yield calculated in *inactivated* samples without considering PSI inactivation (using actually measured P_m instead of original P_m values recorded prior the inactivation) we must take into account different interpretation of the data, as the quantum yields represents fractions of maximum oxidizable PSI content (which is not equal to total PSI content in *inactivated* samples). Φ_{ND}, representing here the fraction of oxidized P700 from all oxidizable P700 ($P700^+/P700_{OX}$) increased very slowly compared to non-inactivated and it was not saturated even at maximum PAR (Fig. 2f). Due to lack of electron transport regulation at low light intensities, the PSI acceptor side was highly reduced in low light (high Φ_{NA}) both in *control* and *inactivated* samples, but, thanks to buildup of transthylakoid ΔpH, the linear electron transport was down-regulated to prevent the over-reduction of PSI at high light intensities. While in *control* samples Φ_{NA} reached its minimum at moderate light intensities, in *inactivated* samples it decreased slowly even in high light (Fig. 2i).

Gas exchange measurements

A detrimental effect of PSI photoinactivation on overall photosynthesis has been assessed using gas exchange light response curves (Fig. 3a).

Obviously, CO_2 assimilation rate was significantly lower in *inactivated* samples. Although stomatal conductance was somewhat lower (Fig. 3b), g_s values were still too high to be responsible for the significant decrease of photosynthetic rate. Moreover, the intercellular CO_2 concentration c_i (Fig. 3c) were higher in *inactivated* samples compared to *control*, indicating the lower carboxylation efficiency (CO_2 assimilation rate per available CO_2 unit) in *inactivated* samples compared to non-inactivated. We observed also more significant stomata closure in *inactivated* samples in low light, however, plotting the relative stomata openness against relative intercellular CO_2 concentration (Fig. 3d) indicates that stomata closure can be fully explained by an increase of CO_2 concentration inside the leaf.

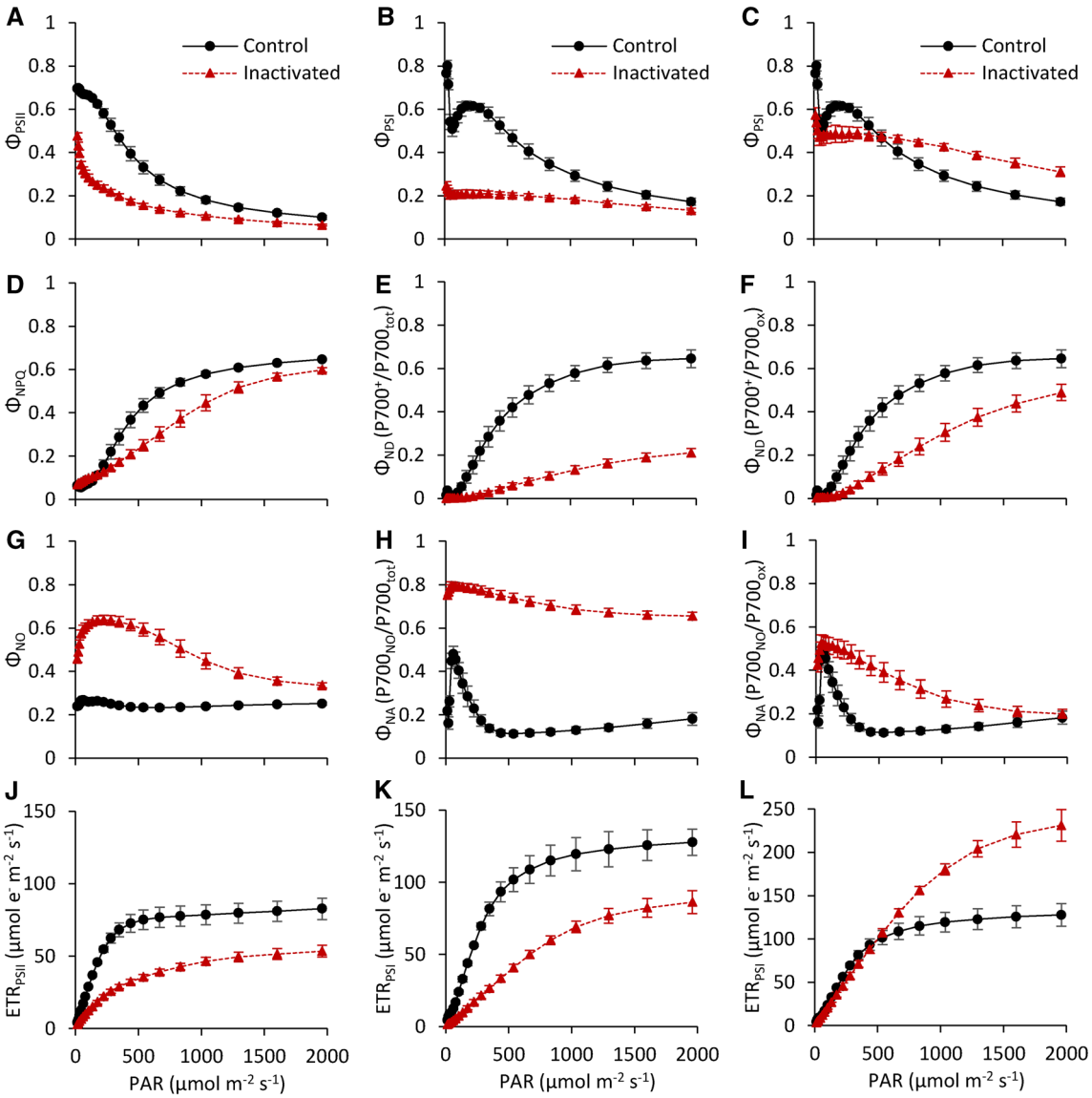

Fig. 2 Light response curves of parameters derived from chlorophyll fluorescence (*column left*), as well as from P700 records measured before PSI inactivation treatment (*Control*) and 2 days after PSI inactivation (*Inactivated*). P700 parameters in *inactivated* samples were calculated either using the initial value of P_m (initial P_m) measured in each sample before PSI inactivation treatment (*middle column*) or using actual P_m values (actual P_m) measured at the beginning of measuring protocol, 2 days after PSI inactivation treatment (*column right*). **a** The effective quantum yield of PSII (Φ_{PSII}). **b** The effective quantum yield of PSI (Φ_{PSI}) calculated using initial P_m. **c** The effective quantum yield of PSI (Φ_{PSI}) calculated using the actual P_m. **d** The quantum yield of regulated non-photochemical quenching in PSII (Φ_{NPQ}). **e** The quantum yield of the PSI non-photochemical quenching caused by the donor-side limitation (Φ_{ND}) calculated using initial P_m, i.e., the fraction of overall P700 that is oxidized in a given state ($P700^+/P700_{TOT}$) and **f** Φ_{ND} calculated using actual P_m, i.e., the fraction of actually oxidizable P700 that is really oxidized in a given state ($P700^+/P700_{OX}$). **g** The fraction of energy captured by PSII passively dissipated in the form of heat and fluorescence (Φ_{NO}). **h** The quantum yield of the PSI non-photochemical quenching caused by the acceptor-side limitation (Φ_{NA}) calculated using initial P_m, i.e., the fraction of overall P700 that cannot be oxidized in a given state ($P700_{NO}/P700_{TOT}$), and **i** Φ_{NA} calculated using actual P_m, i.e., the fraction of oxidizable P700 that cannot be oxidized in a given state ($P700_{NO}/P700_{OX}$). **j** The apparent electron transport rate in PSII (ETR_{PSII}) based on chlorophyll fluorescence measurements. **k** The apparent electron transport rate in PSI (ETR_{PSI}) based on Φ_{PSI} values calculated using initial P_m. **l** The apparent electron transport rate in PSI (ETR_{PSI}) based on Φ_{PSI} values calculated using actual P_m (largely overestimated ETR_{PSI} in *inactivated* samples). The rapid light curves were obtained after previous induction at moderate light; the duration of each interval with a given light intensity was 30 s (see "Materials and methods" section for details). The average values ± SEs from six plants are presented

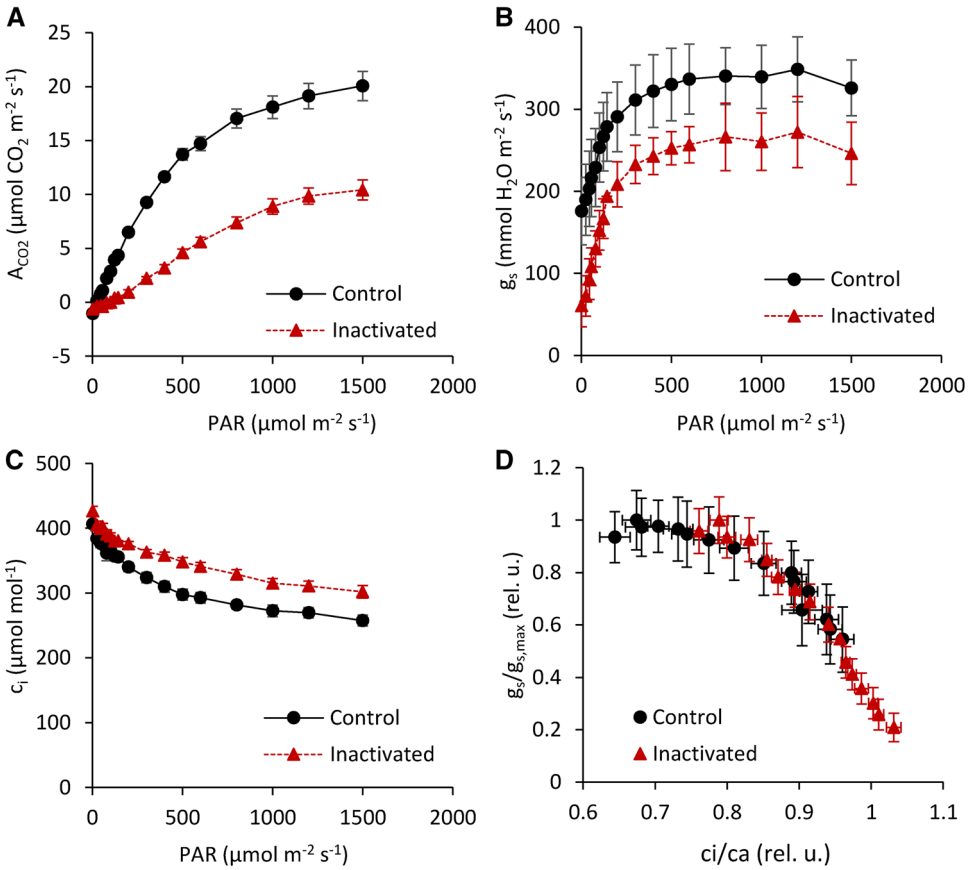

Fig. 3 **a** CO_2 assimilation rate-light response curves recorded before and 2 days after PSI inactivation. **b** Stomatal conductance (g_s) at different light levels. **c** Intercellular CO_2 concentration (c_i) at different light intensities. **d** Relative stomatal openness (expressed as the ratio of actual g_s to maximum $g_{s,\,max}$) related to intercellular to air CO_2 concentration ratio (c_i/c_a). The light curves were recorded after reaching a full stomata openness (steady-state), starting with the highest light level, decreasing stepwise, thus ensuring sufficient enzyme activation level for the next light level (see "Materials and methods" section for details). The average values ± SEs from six plants are presented

The net CO_2 assimilation rate at high light intensities was reduced by ~45 % in *inactivated* samples; however, in low light, the decrease of net assimilation rate due to PSI inactivation was even 75 %. The difference between treatments in respiration rate were not significant, but the quantum yield of CO_2 assimilation decreased from 0.42 in *control* to 0.12 in *inactivated* samples (Supplementary Fig. 1k). The light compensation point was ~32 µmol photons m^{-2} s^{-1} in *control* but ~113 µmol photons m^{-2} s^{-1} in *inactivated* samples. The steep linear increase of A_{CO_2}, indicating electron transport-limited (i.e., light limited) part of the light response curve was limited by the level approximately 150 µmol photons m^{-2} s^{-1} in *control*, but almost 1000 µmol photons m^{-2} s^{-1} in *inactivated* samples (Fig. 3a).

Electrochromic bandshift

The measurements of the dark interval relaxation kinetics of ECS were done on samples illuminated by moderate light intensity (~200 µmol photons m^{-2} s^{-1}) for 15 min, to reach the steady state. We found some obvious differences in the shape of ECS decay induced by switch-off of the actinic light (Supplementary Fig. 2) and ECS parameters (Fig. 4).

In addition to some decrease of the amplitude of the ECS signal (ECS_t), which is considered to be a rough estimate of total total proton motive force (pmf), we observed also differences in new steady value (approximately 20 s after actinic light was switched off). As this value can be used for estimation of two components of pmf (electric component $\Delta\psi_{pmf}$ and osmotic component ΔpH_{pmf}), even visually can be distinguished increase of $\Delta\psi_{pmf}$ and decrease of ΔpH_{pmf} in *inactivated* samples compared to *control*. The numerical values of all parameters derived from ECS decay at both actinic light levels confirm this trend (Fig. 4). The most significant was the decrease of proton gradient (ΔpH_{pmf}) in *inactivated* samples (Fig. 4c). This decrease was partly compensated by an increase of $\Delta\psi_{pmf}$ (Fig. 4b); however, we found some decrease in total pmf due to PSI inactivation (Fig. 4a). The proton conductance, calculated as a time constant of an exponential decay of ECS signal, was almost unaffected by inactivation (Fig. 4d).

Discussion

The PSI photoinhibition in higher plants has been well known for many years, however, it was thought to be limited mostly to the low temperature conditions (Sonoike

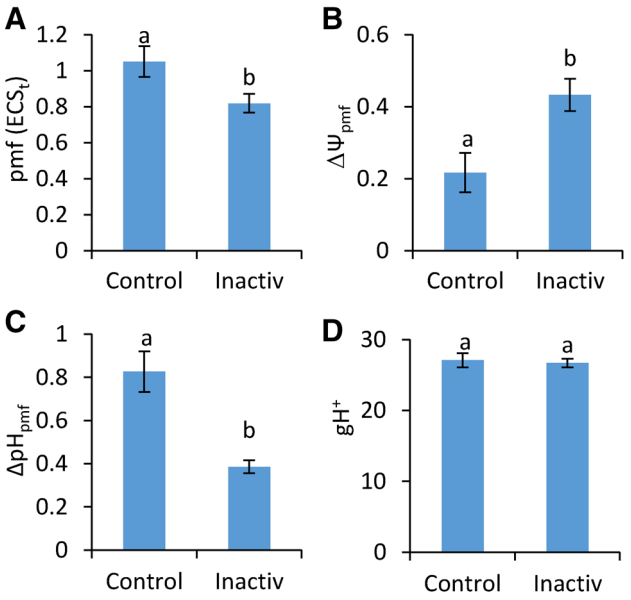

Fig. 4 Parameters derived from the dark-interval relaxation kinetics of ECS ($DIRK_{ECS}$) recorded after 15 min illumination of leaves by red actinic light at ~200 µmol m^{-2} s^{-1} in wheat leaves before PSI inactivation treatment (*Control*) and two days after PSI inactivation (*Inactive*). **a** The amplitude of ECS decay (ECS_t) as an estimate of proton motive force (pmf). **b** The electrical component on total pmf ($\Delta\Psi_{pmf}$). **c** The osmotic component of pmf (ΔpH_{pmf}) estimated from slow ECS kinetics. **d** The tylakoid H^+ conductivity (gH^+) estimated as the reciprocal value of the halftime of the fast ECS decay. The statistically significant differences between *control* and drought-stressed samples at individual light intensities are indicated by the lowercase letters above columns (ANOVA, Tukey HSD test; $P < 0.05$)

2011). However, recent studies have shown that the PSI inactivation may occur in many cases, in which the linear electron transport is not properly regulated due to mutations (Suorsa et al. 2012; Grieco et al. 2012; Tikkanen et al. 2012, 2014) or fluctuating light conditions (Kono et al. 2014; Kono and Terashima 2014). Although the PSI inactivation treatment used in our experiment cannot be regarded as a simulation of naturally occurred phenomenon, it is particularly interesting, but also striking, that several short SP (commonly used in measuring of chlorophyll fluorescence parameters for decades) can drastically affect photosynthetic assimilation in normal, healthy leaves. On the other hand, it gives us a unique opportunity to study the specific effects of PSI photoinhibition in vivo.

Our results have shown, in fact, two main effects of PSI photoinhibition: (1) changes in photochemical processes, associated with electron flow, its regulation and, hence, photoprotective responses, as well as (2) decrease in CO_2 assimilation rate, not caused by the activity of stomata. Even these two issues are closely related, we will discuss them separately in following subchapters.

Effects of PSI photoinactivation on photosynthetic electron transport

In accordance with the results of Sejima et al. (2014) the SP treatment affected PSI more than PSII photochemistry; moreover, PSII quantum yield was partly recovered within a few minutes after SP treatment was stopped and then fully restored in the next days, whereas in the case of PSI we did not observe any recovery even 48 h after SP treatment. Slow recovery was observed by numerous authors studying PSI photoinhibition (Kudoh and Sonoike 2002; Zhang and Scheller 2004). Surprisingly, the full recovery of PSI in our experiment was not obtained even 12 days after SP treatment; the extremely slow PSI recovery can be associated with relatively high light conditions (~300 µmol photons m^{-2} s^{-1}) in growth chamber, as Zhang et al. (2011) have shown that PSI recovery is much faster in a very low light, but very slow recovery at ambient light intensities. Our data also indicated that there were no major differences in photosynthetic responses during the first 3 days after PSI inactivation (Supplementary Fig. 1).

The fast recovery of PSII and slow recovery of PSI would be expected to generate an imbalance in electron distribution between PSII and PSI (Zhang and Scheller 2004). An efficient way to screen the balance between PSI and PSII is a comparison of the light responses of the redox poises at PSII acceptor side and PSI donor side, as in well-balanced systems, the symmetric increase of Q_A^-/Q_A and $P700^+/P700$ (due to "bottleneck effect" of cyt b_6f) can be expected (Cardol et al. 2011; Zivcak et al. 2014b). Our results confirm the predicted trend (Fig. 5), as we observed much faster increase of $Q_A^-/Q_{A,\,TOT}$ in *inactivated* sample compared to *control* (Fig. 5a), whereas the accumulation of oxidized $P700^+$ appeared at moderate light intensities and increased slowly in *inactivated* samples (Fig. 2f). Therefore, the relationship between $Q_A^-/Q_{A,TOT}$ and $P700^+/P700_{OX}$ (Fig. 5b) indicates an almost symmetrical increase of PSII and PSI redox poises in *control* samples, but a strong initial accumulation of reduced electron carriers at the PSII acceptor side without any increase in $P700^+$.

Thus, despite the fully recovered PSII activity of dark-relaxed samples, the light responses of parameters related to PSII photochemistry were affected by PSI inactivation to the similar extent as PSI parameters (Fig. 2). In well-balanced photosynthetic systems (e.g., in our *control* samples), the rate of linear electron transport is down-regulated early to prevent over-reduction of PSI acceptor side (Joliot and Johnson 2011). The downregulation of ETR and increase of NPQ is even faster if the equilibrium between PSII and PSI is displaced in the opposite direction, in favor of PSI (Brestic et al. 2014).

The risk of over-reduction of PSI electron acceptors can be detected by the values of the parameter Φ_{NA} ($P700_{NO}$/

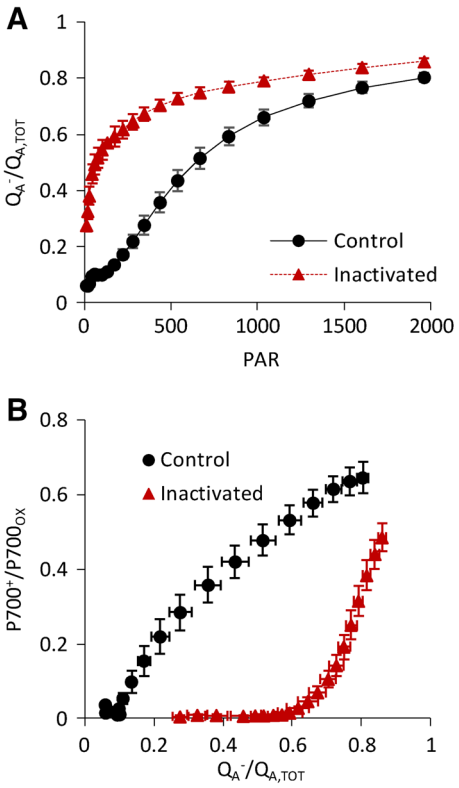

Fig. 5 **a** Redox poise of PSII acceptor side (ratio of reduced Q_A^- to total $Q_{A,\ TOT}$) in samples exposed to different actinic light intensities. **b** Relationship between the redox poise of PSII acceptor side ($Q_A^-/Q_{A,\ TOT}$) and the redox poise of PSI donor side (ratio of oxidized $P700^+$ to all oxidizable $P700_{OX}$) in samples exposed to different actinic light intensities

$P700_{OX}$, Fig. 2i); it is evident, that Φ_{NA} increases quickly, even at relatively low light intensities. The main mechanism of electron transport regulation is the buildup of transthylakoid proton gradient (ΔpH) leading both to down-regulation of electron transport via cyt b_6/f (Heber et al. 1988) and decrease of actual quantum efficiency of PSII by the mechanism called ΔpH-dependent non-photochemical quenching (Weis et al. 1987). Targeting the PSII and PSI parameters, increase in ΔpH led to increase of ΔpH-dependent non-photochemical quenching (NPQ, qE or Φ_{NPQ} parameters), as well as Φ_{ND} parameter indicating the accumulation of $P700^+$ as a result of limited e- supply from PSII due to down-regulated e-transport through cyt b_6/f. In turn, we can use these parameters as an indirect measure of a ΔpH increase. Thus, we can see that in *inactivated* samples, both Φ_{NPQ} and Φ_{ND} (and hence ΔpH) increased much slower than in *control* samples (Fig. 2d, f). As a result, the decrease of Φ_{NA} parameter (Fig. 2i) as a measure of reduction of PSI acceptor side, was much slower and it didn't reach the minimum even at a very high light intensity, indicating insufficient photoprotection of PSI. Moreover, Miyake et al. (2005) found that the PSI photoinhibition is avoided when the photooxidation rate of P700 in PSI exceeds the reduction rate of P700; this was not the case of *inactivated* samples.

The quantum yield of PSII (Fig. 2a) in *control* samples decreased due to increase of ΔpH-dependent non-photochemical quenching (Φ_{NPQ}); however, the decrease of Φ_{PSII} was much steeper than increase of Φ_{NPQ} in *inactivated* samples. It means that the decrease of Φ_{PSII} was not a result of active regulation through buildup of ΔpH across the thylakoid membrane, but resulted simply from overreduction of PSII acceptor side (early increase of $Q_A^-/Q_{A,TOT}$) mentioned above, leading to increase of non-regulated non-photochemical dissipation at PSII (Φ_{NO}) at low and moderate light intensities (Fig. 2g). Φ_{NO} represents energy partitioning through other constitutive processes involved in energy dissipation (Szyszka et al. 2007). Ivanov et al. (2008) suggest that higher Φ_{NO} is associated with increased probability for an alternative non-radiative $P680^+Q_A^-$ radical pair recombination pathway for energy dissipation within the reaction center of PSII (reaction center quenching), as an additional quenching mechanism. In our case, at higher light intensities, with an increase of regulated dissipation (Φ_{NPQ}), the non-regulated dissipation (Φ_{NO}) decreased (Fig. 2d, g).

To summarize the previous discussion, we can say that one of the most important effects of PSI inactivation was the insufficient formation of trans-thylakoid proton gradient. This phenomenon was confirmed also by the analyses of ECS_t decay (Fig. 4). The question is, why?

In the thylakoid membranes of chloroplasts, light-driven electron transport is coupled with the establishment of a proton (H^+) gradient (ΔpH), which together with the membrane potential ($\Delta\psi$), constitutes the total proton motive force (pmf) used to drive chloroplast ATP synthase (Witt 1979; Fischer and Gräber 1999). The size of the proton gradient is determined by the balance between its generation, which depends on photosynthetic electron transport, and its relaxation, which depends mainly on ATP synthase activity (Sacksteder et al. 2000). As the ATP synthase activity (estimated by gH^+ parameter, Fig. 4d, h) was not severely affected by PSI inactivation (at least at moderate light intensities), lower electron transport rate, limited by low PSI content at low-to-moderate light intensity, led to low ΔpH_{pmf}.

In *inactivated* samples, PSI content limits the electron transport rate and thus limits the generation of ΔpH. To ensure sufficient pmf to ATP synthesis, the membrane electric potential is up-regulated (Fig. 4c, g), as ΔpH and $\Delta\psi$ are thermodynamically and kinetically equivalent Mitchel (1966). In contrary, in *control* samples was $\Delta\psi$ very low, in accordance with published observations (Klughammer et al. 2013).

Formation of ΔpH depends on both linear and PSI CET (Munekage et al. 2004; Wang et al. 2015). Using the

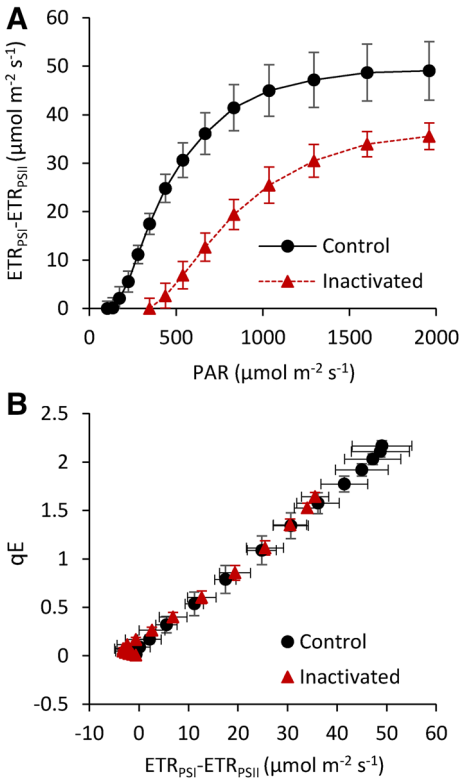

Fig. 6 **a** The rate of cyclic electron transport around PSI estimated as a difference between PSI and PSII electron transport rate (values close to zero recorded in low light are not shown). **b** Relationship between estimated values of PSI cyclic electron flow and ΔpH dependent non-photochemical quenching (qE). In both graphs, the data from simultaneous records of chlorophyll fluorescence and P700 (rapid light curves shown in Fig. 2) are used

difference of PSI and PSII electron transport rate as a rough estimate of the CET rate, it is obvious that CET was triggered at much higher light intensity in *inactivated* samples than in *control*; moreover, the lower maximum CET was achieved (Fig. 6a).

Our results (Fig. 6b) support the importance of CET in formation of ΔpH (Wang et al. 2015), as the estimated rates of CET in *control* and *inactivated* samples were linearly correlated with a fast relaxing component of non-photochemical quenching ratio (qE), which is strongly ΔpH-dependent (Briantais et al. 1979; Ruban et al. 1992). This relationship also suggests that the capacity to reach high CET rate was decreased due to PSI inactivation. Therefore, the contribution of cyclic electron flow seemed to be insufficient to reach transthylakoid proton gradient needed to reach full NPQ in *inactivated* samples.

At this point, it is necessary to mention that the incorrect handling of the measured P700 data may lead to a completely opposite conclusion on the significant enhancement of cyclic electron flow. Indeed, the plots of Φ_{PSI} calculated using actually measured (not initial) values of P_m in *inactivated* samples (Fig. 2c) are rather confusing, as it indicates higher Φ_{PSI} at moderate and high light intensities compared to *control*. More evident is this trend, when these Φ_{PSI} values are used for calculation of ETR_{PSI} using standard formula, without considering the presence of inactivated PSI (Fig. 2l). Thus, ETR_{PSI} at high light intensities seemed to be more than four times higher than ETR_{PSII}. Obviously, the values of Φ_{PSI} and ETR_{PSI} are strongly overestimated, which might lead to the erroneous conclusion that the CET rate was significantly (enormously) enhanced. In this regard, there is reason to suppose that any PSI inactivation, which would take place even a few days prior the measurements (e.g., due to cold stress or fluctuating light), may cause problems to calculate correctly Φ_{PSI}, thus resulting in misinterpretation of the measured data.

Effects of PSI photoinactivation on CO_2 assimilation

The photochemical processes running at the thylakoid membranes are interconnected with the Calvin cycle by the intermediate products, ATP and NADPH, production of which strongly depends on photosynthetic electron transport rate as well as activities of enzymes (ATP synthase, FNR). Therefore, some decrease of CO_2 assimilation rate can be expected as a result of the decrease of PSI photochemical activity; nevertheless, the level of decrease of CO_2 assimilation rate observed repeatedly within our experiments was quite surprising (Fig. 3a). The CO_2 assimilation can be limited both by stomatal closure and by metabolic (non-stomatal) effects (Jones 1985; Zivcak et al. 2013). Although we have observed some decrease of stomatal conductance (Fig. 3b), decrease of CO_2 assimilation can be hardly explained by an effect of stomata, as the g_s values were high enough to ensure sufficient CO_2 uptake, especially at high light levels; moreover, the intercellular CO_2 concentration was higher in *inactivated* leaves compared to *control*, indicating clearly non-stomatal limitation of photosynthesis.

In addition to limited maximum CO_2 assimilation, we observed a serious decrease in maximum quantum yield of CO_2 assimilation (Supplementary Fig. 1k). This parameter is a function of (i) the efficiency of energy transduction into NADPH and ATP on the photosynthetic membrane and (ii) the metabolic pathways in which this reducing and phosphorylating potential is utilized. At current atmospheric CO_2 concentrations, healthy C3 plants show Φ_{CO_2} approximately 0.042 (Long and Drake 1991), which was exactly the same value as we have observed in *control* samples. In *inactivated* samples we observed Φ_{CO_2} between 0.012 and 0.014 (i.e., 70 % lower). Thus, interestingly, decrease of CO_2 quantum yield due to PSI photoinactivation was higher than decrease of photooxidizable PSI content, but it corresponds to a decrease in Φ_{PSI} in low light (Fig. 2).

The initial, linear part of CO_2 light response curve represents the light-limited, i.e., the electron transport-limited part (Ögren and Evans 1993). Typically, the linear part is identified in a range of low light intensity; however, in *inactivated* samples, the electron transport-limited part extended into the high light level (Fig. 3a). It means that in this part of light response curve, the supply of NADPH and/or ATP was not sufficient to saturate metabolic needs. NADPH production depends on linear electron transport, which can be monitored through chlorophyll fluorescence measurements. Interestingly, the steep (light-limited) increase of linear electron transport finished at ~300 µmol photons m^{-2} s^{-1}, after which the linear electron flow in *inactivated* samples was regulated by the ΔpH-dependent mechanisms mentioned above. This regulation was not reflected in CO_2 assimilation, as the steep increase of CO_2 assimilation was still present at much higher light intensities. It means that the NADPH production was not a limiting factor of CO_2 assimilation at high light intensities. On the other hand, PSI electron transport rate (ETR_{PSI}) increased linearly until high light intensities (over 1000 µmol photons m^{-2} s^{-1}) with increasing contribution of CET, which was expected to contribute to proton transport and, hence, to the improvement of the ATP/NADPH ratio, which is critical for meeting of metabolic needs (Kramer et al. 2003).

To compare the effect of PSI inactivation on CO_2 assimilation rate and PSI quantum yield (and hence ETR_{PSI}), we plotted relative values of both parameters compared to *control* samples (Fig. 7).

The graph highlights two important points: (1) The photosynthetic rate at low light intensities was more affected by PSI inactivation than in high light. (2) CO_2 assimilation seems to be limited by the PSI quantum yield up to light intensity ~600 µmol photons m^{-2} s^{-1}. Despite no more electron-transport limitation, CO_2 assimilation at high light intensities was not increasing closer to the value of *control* samples, but it was saturated at the level ~55 % of *control*.

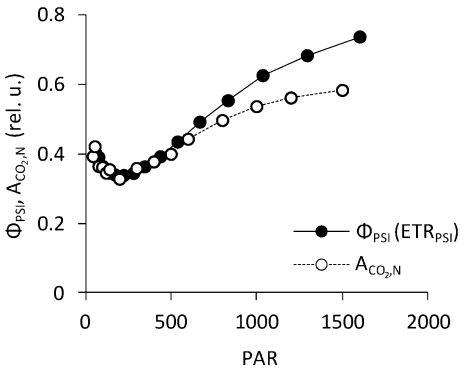

Fig. 7 Average relative values of PSI quantum yield (Φ_{PSI}) or PSI electron transport rate (ETR_{PSI}) and net CO_2 assimilation rate (A_{CO_2}) related to different actinic light intensities. The relative values were calculated as the ratio of values measured in *inactivated* samples to values measured in *control* samples

(1) The severe decrease of photosynthetic performance in low light conditions due to PSI photoinhibition can be a serious problem, as the most probable objects of PSI photoinactivation in natural conditions are the shaded leaves exposed to frequent sunflecks, i.e., strong light pulses in natural environments. Shaded leaves may receive even several hundred of sunflecks per day, mostly shorter than 10 s (Chazdon 1988; Pearcy et al. 1994). Kono et al. (2014) have demonstrated that fluctuating light conditions, i.e., consecutive sunflecks of alternating low- and high-light, caused significant PSI photoinhibition even in wild-type *Arabidopsis* plants. Moreover, PSI photoinhibition in conditions of low temperature is induced by low light (Terashima et al. 1994; Sonoike and Terashima 1994); thus the shaded parts of plant canopies are more endangered, again. The significant increase of light compensation point (Supplementary Fig. 1k) may cause substantial decrease or a complete loss of photosynthetic production in lower leaf positions, with major implications for the whole plant.

(2) An important information is that PSI inactivation and the resulting insufficient number of PSI RCs cannot explain a low CO_2 assimilation rate at high light intensities. As we have excluded the effect of stomata (see "Discussion " section above), the most probable reason of low CO_2 assimilation is decrease of activity of enzyme(s) involved in carbon fixation metabolic pathways. The method used for PSI inactivation eliminates concomitants; therefore, it is probable that a possible decrease of enzyme activities seems to be directly related to the decrease of PSI activity. Activation of Calvin cycle enzymes is partly regulated both by NADPH/$NADP^+$ ratio and/or ATP/ADP ratio (Dietz and Pfannschmidt 2011); however, as we have mentioned before, the activity of ATP synthase and NADPH production seems not to be a key limiting factor in high light conditions in *inactivated* samples. The second mechanism directly related to PSI is regulation of activity of photosynthetic enzymes via thioredoxin/ferredoxin system (Wolosiuk and Buchanan 1977) In addition to reduction of $NADP^+$, the photosynthetic electron flux also reduces thioredoxin (Trx), which, in turn, reduces and activates several enzymes of the Calvin–Benson cycle, especially glyceraldehyde-3-phosphate dehydrogenase (GAPDH), fructose-1,6-bisphosphatase

(FBPase), phosphoribulokinase (PRK), and sedoheptulose-1,7-bisphosphatase (SBPase), but also the regulation of other enzymes such as NADP-dependent malate dehydrogenase (NADP-MDH), chloroplast glucose-6-phosphate dehydrogenase (G6PDH) and many others (Wolosiuk and Buchanan 1977; Ruelland and Miginiac-Maslow 1999; Lemaire et al. 2007; Schürmann and Buchanan 2008; Chibani et al. 2010). Aside from glucose 6-phosphate dehydrogenase, which is reductively deactivated by thioredoxin, each of of the Calvin–Benson cycle enzymes is (directly or indirectly) activated on reduction by thioredoxin (Buchanan et al. 2002). The molecular and structural bases of the Trx-dependent regulation of these enzymes have been investigated in great detail. Carbon metabolism enzymes are strictly regulated by light-dependent thioredoxins reduced by electrons from PSI (Trx_f and Trx_m), enabling a finely tuned day/light regulation of carbon metabolism (Meyer et al. 2012). In our experiment, we have shown that PSI acceptor side is strongly affected by PSI inactivation (Fig. 2h), which may be the cause of insufficient thioredoxin reduction, leading to not fully activated enzymes of Calvin cycle. Alternatively, if we assume that the activation of enzymes by Trx at different light intensities depends on PSI electron transport rate, then the ETR_{PSI} slowed down due to PSI inactivation will mimic the lower light level, leading consequently to down-regulation of Calvin cycle to that level. Regardless of the exact mechanism, a lower NADPH demand of the down-regulated Calvin cycle (decrease of NADP+/NADPH ratio) may explain the ΔpH dependent down-regulation of linear electron transport (ETR_{PSII}) in *inactivated* samples at high light conditions (Okegawa et al. 2008). However, the hypothesis on the effect of PSI inactivation on thioredoxin/ferredoxin system-mediated activation of Calvin cycle needs to be verified at the molecular and biochemical level.

Conclusions

The inactivation of PSI caused by a series of short light SP applied by fluorimeter in darkness led to a severe, very slowly relaxing decrease of PSI photochemical activity. It led to an imbalance between PSII and PSI photochemistry, with a high excitation pressure on PSII acceptor side and low oxidation of the PSI donor side. Low activity of PSI was associated with a decrease in formation of transthylakoid proton gradients (ΔpH), and hence, a lower non-photochemical quenching at PSII, as well as highly reduced acceptor side of PSI. In parallel with photochemical parameters, the CO_2 assimilation was also strongly inhibited, more in low light than in high light; the decrease was not caused by stomatal closure. The CO_2 assimilation was limited by the PSI electron transport supply at low to moderate light intensities, but at high light, carboxylation rate seemed to be decreased due to down-regulated activity of Calvin cycle enzymes, which is fine-tuned by the redox signaling at the PSI acceptor side.

Acknowledgments This work was supported by the European Community under the project no. 26220220180: "Construction of the "AgroBioTech" Research Centre and project "Center of Excellence for Agrobiodiversity Conservation and Use, ECOVA"." SIA was supported by Grants from the Russian Foundation for Basic Research (Nos. 14-04-01549, 14-04-92690), and by Molecular and Cell Biology Programs of the Russian Academy of Sciences.

References

Alboresi A, Ballottari M, Hienerwadel R, Giacometti GM, Morosinotto T (2009) Antenna complexes protect photosystem I from photoinhibition. BMC Plant Biol 9:71

Allakhverdiev SI, Murata N (2004) Environmental stress inhibits the synthesis de novo of proteins involved in the photodamage-repair cycle of Photosystem II in *Synechocystis* sp. PCC 6803. Biochim Biophys Acta 1657:23–32

Allakhverdiev SI, Murata N (2008) Salt stress inhibits photosystems II and I in cyanobacteria. Photosynth Res 98:529–539

Apostol S, Briantais JM, Moise N, Cerovic Z, Moya I (2001) Photoinactivation of the photosynthetic electron transport chain by accumulation of over-saturating light pulses given to dark adapted pea leaves. Photosynth Res 67:215–227

Baker NR (2008) Chlorophyll fluorescence: a probe of photosynthesis *in vivo*. Annu Rev Plant Biol 59:89–113

Barber J, Andersson B (1994) Revealing the blueprint of photosynthesis. Nature 370:31–34

Brestic M, Zivcak M, Olsovska K, Shao HB, Kalaji HM, Allakhverdiev SI (2014) Reduced glutamine synthetase activity plays a role in control of photosynthetic responses to high light in barley leaves. Plant Physiol Biochem 81:74–83

Briantais JM, Vernotte C, Picaud M, Krause GH (1979) A quantitive study of the slow decline of chlorophyll a fluorescence in isolated chloroplasts. Biochim Biophys Acta 548:128–138

Buchanan BB, Schürmann P, Wolosiuk RA, Jacquot JP (2002) The ferredoxin/thioredoxin system: from discovery to molecular structures and beyond. Photosynth Res 73:215–222

Bukhov NG, Carpentier R (2003) Measurement of photochemical quenching of absorbed quanta in photosystem I of intact leaves using simultaneous measurements of absorbance changes at 830 nm and thermal dissipation. Planta 216:630–638

Bukhov N, Carpentier R (2004) Alternative photosystem I-driven electron transport routes: mechanisms and functions. Photosynth Res 82:17–33

Cardol P, Forti G, Finazzi G (2011) Regulation of electron transport in microalgae. Biochim Biophys Acta 1807:912–918

Chazdon R (1988) Sunflecks and their importance to forest understory plants. Adv Ecol Res 18:1–63

Chibani K, Couturier J, Selles B, Jacquot JP, Rouhier N (2010) The chloroplastic thiol reducing systems: dual functions in the regulation of carbohydrate metabolism and regeneration of

antioxidant enzymes, emphasis on the poplar redoxin equipment. Photosyn Res 104:75–99

Demmig-Adams B (1990) Carotenoids and photoprotection in plants: a role for the xanthophyll zeaxanthin. Biochim Biophys Acta 1020:1–24

Dietz KJ, Pfannschmidt T (2011) Novel regulators in photosynthetic redox control of plant metabolism and gene expression. Plant Physiol 155:1477–1485

Fischer S, Gräber P (1999) Comparison of ΔpH- and Δφ-driven ATP synthesis catalyzed by H + -ATPases from Escherichia coli or chloroplasts reconstituted into liposomes. FEBS Lett 457:327–332

Goltsev V, Zaharieva I, Chernev P, Kouzmanova M, Kalaji MH, Yordanov I, Krasteva V, Alexandrov V, Stefanov D, Allakhverdiev SI, Strasser RJ (2012) Drought-induced modifications of photosynthetic electron transport in intact leaves: analysis and use of neural networks as a tool for a rapid non-invasive estimation. Biochim Biophys Acta 1817:1490–1498

Grieco M, Tikkanen M, Paakkarinen V, Kangasjärvi S, Aro EM (2012) Steady-state phosphorylation of light-harvesting complex II proteins preserves Photosystem I under fluctuating white light. Plant Physiol 160:1896–1910

Heber U, Neimanis S, Dietz KJ (1988) Fractional control of photosynthesis by the QB-protein, the cytochrome-f cytochrome-B6 complex and other components of the photosynthetic apparatus. Planta 173:267–274

Ivanov AG, Morgan R, Gray G, Velitchkova M, Huner NP (1998) Temperature/light dependent development of selective resistance to photoinhibition of photosystem I. FEBS Lett 430:288–292

Ivanov AG, Krol M, Zeinalov Y, Huner NPA, Sane PV (2008) The lack of LHCII proteins modulates excitation energy partitioning and PSII charge recombination in Chlorina F2 mutant of barley. Physiol Mol Biol Plants 14:205–215

Joliot P, Johnson GN (2011) Regulation of cyclic and linear electron flow in higher plants. Proc Natl Acad Sci USA 108:13317–13322

Joliot P, Joliot A (2002) Cyclic electron transfer in plant leaf. Proc Natl Acad Sci USA 99:10209–10214

Jones HG (1985) Partitioning stomatal and non-stomatal limitations to photosynthesis. Plant Cell Environ 8:95–104

Kalaji HM, Schansker G, Ladle RJ, Goltsev V, Bosa K, Allakhverdiev SI et al (2014) Frequently asked questions about in vivo chlorophyll fluorescence: practical issues. Photosynth Res 122:121–158

Klughammer C, Schreiber U (1994) Saturation pulse method for assessment of energy conversion in PS I. Planta 192:261–268

Klughammer C, Siebke K, Schreiber U (2013) Continuous ECS-indicated recording of the proton-motive charge flux in leaves. Photosynth Res 117:471–487

Kono M, Terashima I (2014) Long-term and short-term responses of the photosynthetic electron transport to fluctuating light. J Photochem Photobiol B 137:89–99

Kono M, Noguchi K, Terashima I (2014) Roles of the cyclic electron flow around PSI (CEF-PSI) and O_2-dependent alternative pathways in regulation of the photosynthetic electron flow in short-term fluctuating light in *Arabidopsis thaliana*. Plant Cell Physiol 55:990–1004

Kramer DM, Evans JR (2011) The importance of energy balance in improving photosynthetic productivity. Plant Physiol 155:70–78

Kramer DM, Cruz JA, Kanazawa A (2003) Balancing the central roles of the thylakoid proton gradient. Trends Plant Sci 8:27–32

Kramer DM, Johnson G, Kiirats O, Edwards GE (2004) New fluorescence parameters for the determination of QA redox state and excitation energy fluxes. Photosynth Res 79:209–218

Kudoh H, Sonoike K (2002) Irreversible damage to photosystem I by chilling in the light: cause of the degradation of chlorophyll after returning to normal growth temperature. Planta 215:541–548

Lemaire SD, Michelet L, Zaffagnini M, Massot V, Issakidis-Bourguet E (2007) Thioredoxins in chloroplasts. Curr Genet 51:343–365

Li XP, Björkman O, Shih C, Grossman AR, Rosenquist M, Jansson S, Niyogi KK (2000) A pigment-binding protein essential for regulation of photosynthetic light harvesting. Nature 403:391–395

Long SP, Drake BG (1991) Effect of the long-term elevation of CO_2 concentration in the field on the quantum yield of photosynthesis of the C3 sedge, *Scirpus-olneyi*. Plant Physiol 96:221–226

Meyer Y, Belin C, Delorme-Hinoux V, Reichheld JP, Riondet C (2012) Thioredoxin and glutaredoxin systems in plants: molecular mechanisms, crosstalks, and functional significance. Antioxid Redox Signal 17:1124–1160

Mitchell P (1966) Chemiosmotic coupling in oxidative and photosynthetic phosphorylation. Biol Rev 41:445–502

Miyake C (2010) Alternative electron flows (water–water cycle and cyclic electron flow around PSI) in photosynthesis: molecular mechanisms and physiological functions. Plant Cell Physiol 51:1951–1963

Miyake C, Miyata M, Shinzaki Y, Tomizawa KI (2005) CO_2 response of cyclic electron flow around PSI (CEF-PSI) in tobacco leaves—relative electron fluxes through PSI and PSII determine the magnitude of non-photochemical quenching (NPQ) of Chl fluorescence. Plant Cell Physiol 46:629–637

Munekage Y, Hashimoto M, Miyake C, Tomizawa KI, Endo T, Tasaka M, Shikanai T (2004) Cyclic electron flow around photosystem I is essential for photosynthesis. Nature 429:579–582

Murata N, Takahashi S, Nishiyama Y, Allakhverdiev SI (2007) Photoinhibition of photosystem II under environmental stress. Biochim Biophys Acta 1767:414–421

Ögren E, Evans JR (1993) Photosynthetic light-response curves. Planta 189:182–190

Okegawa Y, Kagawa Y, Kobayashi Y, Shikanai T (2008) Characterization of factors affecting the activity of photosystem I cyclic electron transport in chloroplasts. Plant Cell Physiol 49:825–834

Pearcy RW, Chazdon RL, Gross LJ, Mott KA (1994) Photosynthetic utilization of sunflecks: a temporally patchy resource on a time scale of seconds to minutes. In: Caldwell MM, Pearcy RW (eds) Exploitation of environmental heterogeneity by plants. Academic Press, San Diego, pp 175–208

Powles SB (1984) Photoinhibition of Photosynthesis Induced by Visible Light. Annu Rev Plant Physiol 35:15–44

Purcell M, Carpentier R (1994) Homogeneous photobleaching of chlorophyll holochromes in a photosystem I reaction center complex. Photochem Photobiol 59:215–218

Rajagopal S, Bukhov NG, Carpentier R (2002) Changes in the structure of chlorophyll-protein complexes and excitation energy transfer during photoinhibitory treatment of isolated photosystem I submembrane particles. J Photochem Photobiol B 62:194–200

Rajagopal S, Bukhov NG, Carpentier R (2003) Photoinhibitory light-induced changes in the composition of chlorophyll-protein complexes and photochemical activity in photosystem-I submembrane fractions. Photochem Photobiol 77:284–291

Ruban AV, Walters RG, Horton P (1992) The molecular mechanism of the control of excitation energy dissipation in chloroplast membranes inhibition of pH-dependent quenching of chlorophyll fluorescence by dicyclohexylcarbodiimide. FEBS Lett 309:175–179

Ruelland E, Miginiac-Maslow M (1999) Regulation of chloroplast enzyme activities by thioredoxins: activation or relief from inhibition? Trends Plant Sci 4:136–141

Sacksteder CA, Kramer DM (2000) Dark-interval relaxation kinetics (DIRK) of absorbance changes as a quantitative probe of steady-state electron transfer. Photosynth Res 66:145–158

Sacksteder CA, Kanazawa A, Jacoby ME, Kramer DM (2000) The proton to electron stoichiometry of steady-state photosynthesis in

living plants: a proton-pumping Q-cycle is continuously engaged. Proc Natl Acad Sci USA 97:14283–14288
Scheller HV, Haldrup A (2005) Photoinhibition of photosystem I. Planta 221:5–8
Schürmann P, Buchanan BB (2008) The ferredoxin/thioredoxin system of oxygenic photosynthesis. Antioxid Redox Signal 10:1235–1274
Sejima T, Takagi D, Fukayama H, Makino A, Miyake C (2014) Repetitive short-pulse light mainly inactivates photosystem I in sunflower leaves. Plant Cell Physiol. doi:10.1093/pcp/pcu061
Shen Y-K, Chow WS, Park Y-I, Anderson JM (1996) Photoinactivation of Photosystem II by cumulative exposure to short light pulses during the induction period of photosynthesis. Photosynth Res 47:51–59
Shikanai T (2012) Cyclic electron transport around photosystem I; genetic approaches. Annu Rev Plant Biol 58:199–217
Shikanai T (2014) Central role of cyclic electron transport around photosystem I in the regulation of photosynthesis. Curr Opin Biotechnol 26:25–30
Sonoike K (1996) Photoinhibition of photosystem I: its physiological significance in the chilling sensitivity of plants. Plant Cell Physiol 37:239–247
Sonoike K (2011) Photoinhibition of photosystem I. Physiol Plant 142:56–64
Sonoike K, Terashima I (1994) Mechanism of photosystem-I photoinhibition in leaves of *Cucumis sativus* L. Planta 194:287–293
Sonoike K, Kamo M, Hihara Y, Hiyama T, Enami I (1997) The mechanism of the degradation of PsaB gene product, one of the photosynthetic reaction centre subunits of photosystem I, upon photoinhibition. Photosynth Res 53:55–63
Suorsa M, Jarvi S, Grieco M, Nurmi M, Pietrzykowska M, Rantala M, Kangasjarvi S, Paakkarinen V, Tikkanen M, Jansson S, Aro EM (2012) Proton gradient regulation5 is essential for proper acclimation of *Arabidopsis* photosystem I to naturally and artificially fluctuating light conditions. Plant Cell 24:2934–2948
Szyszka B, Ivanov AG, Huner NP (2007) Psychrophily is associated with differential energy partitioning, photosystem stoichiometry and polypeptide phosphorylation in *Chlamydomonas raudensis*. Biochim Biophys Acta 1767:789–800
Teicher HB, Møller BL, Scheller HV (2000) Photoinhibition of photosystem I in field-grown barley (*Hordeum vulgare* L.): induction, recovery and acclimation. Photosynth Res 64:53–61
Terashima I, Funayama S, Sonoike K (1994) The site of photoinhibition in leaves of *Cucumis sativus* L. at low temperatures is photosystem I, not photosystem II. Planta 193:300–306
Thiele A, Winter K, Krause GH (1997) Low inactivation of D1 protein of photosystem II in young canopy leaves of Anacardium excelsum under high-light stress. J Plant Physiol 151:286–292
Tikkanen M, Grieco M, Nurmi M, Rantala M, Suorsa M, Aro EM (2012) Regulation of the photosynthetic apparatus under fluctuating growth light. Philos Trans Roy Soc B 367:3486–3493
Tikkanen M, Mekala NR, Aro EM (2014) Photosystem II photoinhibition-repair cycle protects Photosystem I from irreversible damage. Biochim Biophys Acta 1837:210–215
Tjus SE, Møller BL (1998) Scheller HV (1998) Photosystem I is an early target of photoinhibition in barley illuminated at chilling temperatures. Plant Physiol 116:755–764
Tjus SE, Møller BL, Scheller HV (1999) Photoinhibition of photosystem I damages both reaction centre proteins PSI-A and PSI-B and acceptor-side located small photosystem I polypeptides. Photosynth Res 60:75–86
Wang LF, Chen YY (2013) Characterization of a wide leaf mutant of rice (*Oryza sativa* L.) with high yield potential in field. Pak J Bot 45:921–926
Wang C, Yamamoto H, Shikanai T (2015) Role of cyclic electron transport around photosystem I in regulating proton motive force. Biochim Biophys Acta. doi:10.1016/j.bbabio.2014.11.013
Weis E, Ball JR, Berry J (1987) Photosynthetic control of electron transport in leaves of Phaseolus vulgaris. Evidence for regulation of PSII by the proton gradient. In: Biggins J (ed) Progress in photosynthesis research. Kluwer, Dordrecht, pp 553–556
Witt HT (1979) Energy conversion in the functional membrane of photosynthesis. Analysis by light pulse and electric pulse methods the central role of the electric field. Biochim Biophys Acta 505:355–427
Wolosiuk RA, Buchanan BB (1977) Thioredoxin and glutathione regulate photosynthesis in chloroplasts. Nature 266:565–567
Zhang S, Scheller HV (2004) Photoinhibition of photosystem I at chilling temperature and subsequent recovery in Arabidopsis thaliana. Plant Cell Physiol 45:1595–1602
Zhang ZS, Jia YJ, Gao HY, Zhang LT, Li HD, Meng QW (2011) Characterization of PSI recovery after chilling-induced photoinhibition in cucumber (*Cucumis sativus* L.) leaves. Planta 234:883–889
Zivcak M, Brestic M, Balatová Z, Drevenaková P, Olsovska K, Kalaji HM, Allakhverdiev SI (2013) Photosynthetic electron transport and specific photoprotective responses in wheat leaves under drought stress. Photosynth Res 117:529–546
Zivcak M, Brestic M, Kalaji HM, Govindjee (2014a) Photosynthetic responses of sun-and shade-grown barley leaves to high light: is the lower PSII connectivity in shade leaves associated with protection against excess of light? Photosynth Res 119:339–354
Zivcak M, Kalaji HM, Shao HB, Olšovská K, Brestič M (2014b) Photosynthetic proton and electron transport in wheat leaves under prolonged moderate drought stress. J Photochem Photobiol B 137:107–115